PHILOSOPHICAL TRANSACTIONS OF THE ROYAL SOCIETY A
MATHEMATICAL, PHYSICAL & ENGINEERING SCIENCES

The H_3^+ ion: a remote diagnostic of the jovian magnetosphere

J. E. P. Connerney and T. Satoh

Phil. Trans. R. Soc. Lond. A 2000 **358**, 2471-2483
doi: 10.1098/rsta.2000.0661

10.1098/rsta.2000.0661

The H_3^+ ion: a remote diagnostic of the jovian magnetosphere

By J. E. P. Connerney[1] and T. Satoh[2]

[1]*Laboratory for Extraterrestrial Physics, Code 695, NASA/GSFC, Greenbelt, MD 20771, USA* (jec@lepjec.gsfc.nasa.gov)

[2]*Frontier Research Center for Computational Sciences, Science University of Tokyo, 2641 Yamazaki, Noda-shi, Chiba 278–8510, Japan*

Observations of the jovian system in the near-infrared (3.4 μm) reveal a wealth of information about Jupiter's magnetic field, magnetosphere, and magnetospheric dynamics. This wavelength contains a few emission lines of the H_3^+ ion *and* it is centred on a deep methane absorption band. As a result, one can image Jupiter's ionosphere at this wavelength with extraordinary signal-to-noise ratio, against a planet otherwise darkened by absorption due to methane in its atmosphere. High spatial resolution images of the planet's surface provide a synoptic view of the entire magnetosphere, from the electrodynamics of Io and the torus, to the excitation of auroral displays at high magnetic latitude. Observations of the Io Flux Tube footprint have provided a new magnetic coordinate system for the jovian polar regions and new insight into the electrodynamic interaction between Jupiter and Io. Short-term temporal variations (days) of auroral intensity are observed in the IR and are well correlated with variations in the solar-wind ram pressure arriving at Jupiter. These H_3^+ emissions are thermally excited and are a good proxy for time-averaged energy deposition. It is now possible to produce detailed maps of energy deposition from the Io footprint ($L = 6$) to the pole, in which both system III and local time variations are evident.

Keywords: infrared; H_3^+; magnetosphere; Jupiter; auroral; Io

1. Introduction

Burke & Franklin (1955) detected low-frequency radio emission from Jupiter in 1955 and initiated an era of remote observation of Jupiter's magnetosphere using radio telescopes. This occurred before the launch of Sputnik in 1957 and prior to the introduction of the term 'magnetosphere' by T. Gold in 1959. By the time the first space probe arrived at Jupiter in 1973, much was already known about Jupiter's magnetic field and the enigmatic interaction between it and the innermost Galilean satellite, Io (see review by Carr *et al.* (1983)). *In situ* observations of the magnetic field and magnetospheric plasmas confirmed the presence of an Earth-like magnetic field, with an axis of symmetry tilted by *ca.* 10° with respect to the rotation axis (reviewed by Acuña *et al.* (1983)). With a magnetic moment of *ca.* 1.5×10^{30} G cm^3, Jupiter is the most magnetic planet in the solar system. At a distance of 5.2 AU from the sun, it creates a voluminous obstacle to the solar wind that would appear in the sky about three times as large as the Moon or Sun.

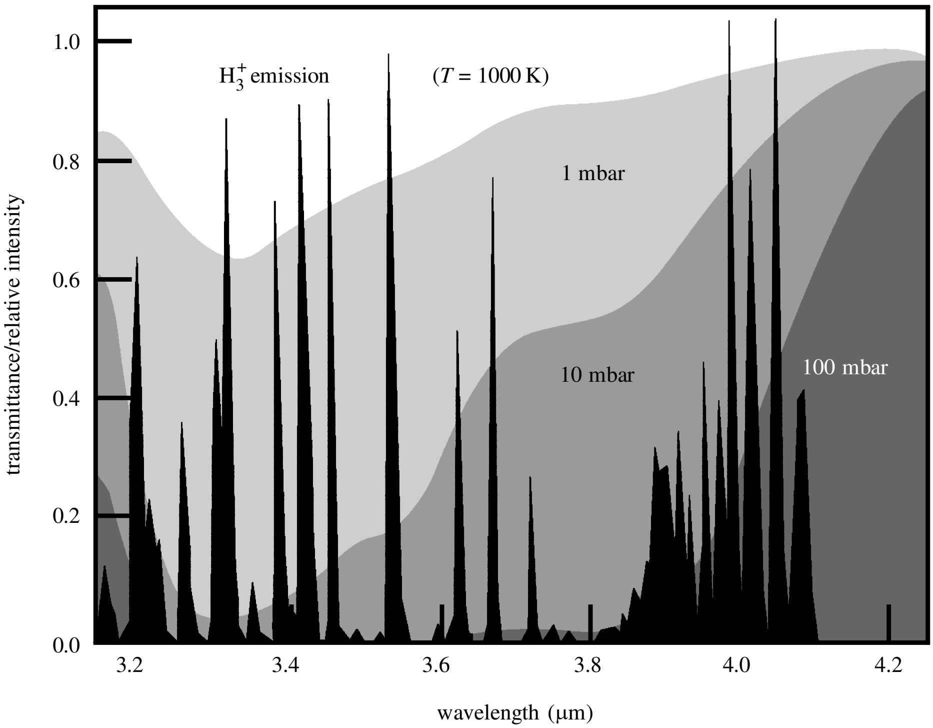

Figure 1. Intensity of H_3^+ emission lines in the L-band atmospheric window and the transmittance of the jovian atmosphere at several pressure levels (1 mbar, 10 mbar, 100 mbar).

Like Earth, Jupiter also has an omnipresent and spectacular auroral display, first observed at ultraviolet (UV) wavelengths by the Voyager spacecraft during its 1979 flyby (Broadfoot *et al.* 1979). Jovian UV spectra are dominated by the intense 1216 Å hydrogen Lyα emission line, followed by H_2 Lyman and Werner band emissions. Ultraviolet spectrometers aboard the Earth-orbiting International Ultraviolet Explorer (IUE) and Hubble Space Telescope (HST) have monitored jovian auroral activity beginning with the IUE observations of Clarke *et al.* (1980). Direct imaging of the UV aurora became possible with the faint object camera (FOC) on the HST in 1992 (Caldwell *et al.* 1992; Dols *et al.* 1992; Gérard *et al.* 1993), and, subsequently, with the wide field planetary camera (WFPC2) on the HST (Clarke *et al.* 1996, 1998; Prangé *et al.* 1998).

Infrared emissions due to the molecular ion H_3^+ were first detected spectroscopically in a 2 μm overtone band (Drossart *et al.* 1989; Trafton *et al.* 1989; Oka & Geballe 1990) and subsequently imaged in the 3–4 μm ν_2 fundamental band using an IR array camera at NASA's 3 m infrared telescope facility (IRTF) (Baron *et al.* 1991; Kim *et al.* 1991). H_3^+ is formed in the jovian ionosphere by the rapid ion–molecule reaction ($H_2^+ + H_2 \rightarrow H_3^+ + H$) that follows ionization of molecular H_2. H_3^+ is the major ionospheric ion between *ca.* 1 and 100 μbar, with H^+ dominating at higher altitudes (Waite *et al.* 1997; Kim & Fox 1994; Achilleos *et al.* 1998). H_3^+ emission originates from a critical region of Jupiter's atmosphere, where the planet electrically couples to its environment, providing a uniquely valuable remote diagnostic of magnetospheric phenomena.

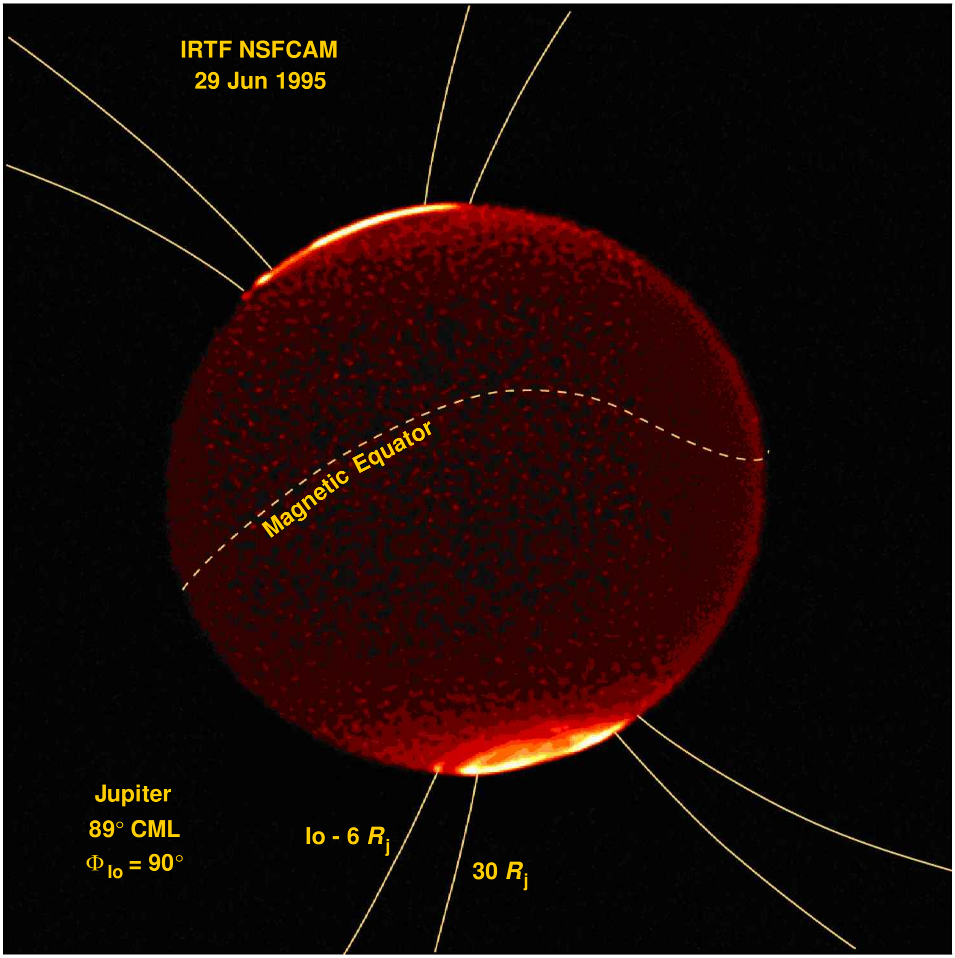

Figure 2. Image of Jupiter at 3.4 μm obtained at NASA's IRTF at Mauna Kea, Hawaii, using the NSFCAM facility imager. At this wavelength, bright H_3^+ emissions appear against a planetary disc darkened by methane absorption.

Imaging and spectroscopy of H_3^+ have, thus, emerged as a valuable probe of Jupiter's atmosphere and magnetosphere. We present here results of the imaging campaigns and refer to a companion article by Miller *et al.* (this issue) who summarize spectroscopic observations of Jupiter. Imaging and spectroscopy are highly complementary. Spectroscopy is more diagnostic of the H_3^+ source region, e.g. to infer temperatures, number densities, and conditions in Jupiter's atmosphere. Imaging is more diagnostic of Jupiter's magnetic field and magnetosphere, its response to the solar wind, and satellite interactions. Together they provide a synoptic view of the state of the jovian magnetosphere.

2. H_3^+ imagery

A plethora of jovian H_3^+ emission lines is available in the near-infrared, particularly in the *K*-band (2–2.5 μm) and *L*-band (3–4 μm) atmospheric windows. To best observe jovian H_3^+ from terrestrial observatories, such as NASA's IRTF atop Hawaii's Mauna Kea volcano, we need to satisfy three constraints. We look for a strong H_3^+ emission line, or group of several lines within the imager bandpass. We need to find emission lines that coincide with terrestrial 'atmospheric windows', i.e. regions of the spectrum relatively free of molecular band absorption, scattering and extinction due to water vapour and atmospheric constituents. These first two constraints can be satisfied throughout much of the K-band and L-band windows. We choose to image a group of H_3^+ emission lines near 3.4 μm to take advantage of a deep methane absorption band (figure 1) that prevents light from deep in Jupiter's atmosphere from escaping. Within this absorption band, Jupiter appears very dark, free of reflected sunlight or other emissions originating below the homopause. Thus, the high-altitude emissions we are interested in appear with extraordinary signal-to-noise (S/N) ratio against a background darkened by absorption due to methane in the well-mixed part of Jupiter's atmosphere (pressures greater than a few millibars).

Figure 2 is a 3.4 μm image of Jupiter taken with the 256 × 256 pixel NSFCAM infrared array camera and the circular variable filter (CVF) at the IRTF. The figure is actually a composite of several images, since Jupiter's disc more than fills the field of view of the telescope. Individual images are acquired with 20 s integrated exposure time (e.g. 10 exposures of 2 s each, co-added) with a S/N ratio of more than 100. These individual images are then cross-correlated and joined to construct full disc images or co-added to further improve the dynamic range. This composite figure shows H_3^+ emissions that have very different origins, which, once deciphered, reveal much about Jupiter's ionosphere and magnetosphere.

The high-latitude emission evident at both poles is the H_3^+ aurora. The greatly increased emission intensity at these latitudes results from the precipitation of energetic charged particles, arriving from the distant magnetosphere along magnetic field lines crossing the Equator between *ca.* 12 and $30 R_j$ radial distance (Satoh & Connerney 1999*a*; Satoh *et al.* 1996). A less intense band of emission extends a few degrees in latitude equatorward from the main oval to the Io L-shell footprint, i.e. those field lines crossing the Equator at the orbital distance of Io. A few million megawatts of power are radiated away from the auroral zone by the H_3^+ ion alone.

The view of Jupiter's auroral ovals changes dramatically as Jupiter rotates, for an observer on Earth, due to the *ca.* 10° angle between Jupiter's magnetic and rotation axes (Connerney 1993). In figure 2, obtained at 89° jovian system III longitude (positive west is the convention, i.e. longitudes increase with time), the southern magnetic pole is tilted towards the observer, so the southern auroral oval is most visible. The variation of auroral intensity with jovian system III longitude approximates a sinusoidal variation (Baron *et al.* 1996) that can be analytically related to the position, size and altitude of the auroral ovals (Connerney *et al.* 1996). Since one can rarely acquire observations over a full rotation (10 h) in a single night, this model is extremely useful in comparing observations from night to night. The integrated intensity of the H_3^+ aurora varies by about a factor of two or three depending on the observer's longitude.

In addition to the prominent auroral emission, an isolated and distinct emission feature can be seen on the dawn limb just a few degrees equatorward of the auroral emission. This feature appears at the foot of the magnetic field line linking Jupiter's ionosphere and the innermost Galilean satellite, Io, orbiting at a radial distance of $5.95 R_j$. It is the surface expression of the electrodynamic interaction between

Jupiter's magnetic field and the satellite. The feature can be seen in both hemispheres, if the viewing geometry allows, and moves across Jupiter's disc in concert with the orbital motion of Io. First detected in the infrared (Connerney *et al*. 1993), it has also been observed in the UV (Clarke *et al*. 1996, 1998; Prangé *et al*. 1998) with instruments aboard the HST. This feature provides a fiducial reference mark on the planet's surface, greatly improving the accuracy of jovian magnetic field models and auroral mapping (Connerney *et al*. 1998). It is also a powerful tool for understanding the detailed nature of the electrodynamic interaction between Jupiter and Io.

The disc of Jupiter can also be seen in figure 2, against a darker background, as it is illuminated by weaker emission from the non-auroral ionosphere. While the disc appears uniformly illuminated in figure 2, if one allows for limb brightening of the emission, spatial variations of the lower-latitude emissions have been mapped spectroscopically (Miller *et al*. 1997; Lam *et al*. 1997). In our images, the majority of the non-auroral H_3^+ appears distributed as one would expect of an ion formed quickly as a result of solar EUV radiation (Satoh & Connerney 1999*b*). The observation of limb brightening and a dark terminator at both dawn and dusk (before and after opposition) argues for rapid recombination of H_3^+, i.e. the H_3^+ density is substantially depleted during *ca.* 5° of jovian rotation (500 s). Using a recombination time constant of $\kappa_r = 2\times10^{-7}\ cm^3\ s^{-1}$ (Leu *et al*. 1973), this implies an electron density of $10^4\ cm^{-3}$ at the altitude of the H_3^+ (non-auroral) disc emissions. This must be well above the altitude of the peak ionospheric electron density (a few times 10^4 to a few times $10^5\ cm^{-3}$) measured by radio occultations at high solar zenith angles (Strobel & Atreya 1983). From the spatial distribution one can deduce that the non-auroral H_3^+ emission peaks at an altitude corresponding to *ca.* 5–7 nbar pressure, consistent with the detailed numerical model of Achilleos *et al*. (1998).

3. Aurora

There is great interest in using auroral emissions to study the dynamics of Jupiter's magnetosphere. The entire magnetosphere can be mapped to the surface of Jupiter with a suitable magnetospheric model. Since particles move freely along magnetic field lines, the ionosphere and magnetosphere are tightly coupled. What we (often) cannot observe in the distant magnetosphere may have a visible (or infrared) expression in the ionosphere that we can study. A visiting space probe, such as Galileo or Ulysses, and Voyagers 1 and 2 before them, can sample a minute fraction of the magnetosphere. *In situ* observations of the magnetic field and charged-particle environment are much more valuable if we can infer how to globalize our local knowledge. Images of the aurora help us do that, since each image is a snapshot of the entire magnetosphere mapped onto the ionosphere.

The ability to associate a location in the ionosphere with its counterpart in the distant magnetosphere depends critically on the accuracy of the magnetic map. The map has two parts: the magnetic field of the planet (Acuña *et al*. 1983; Connerney 1993) and that of the magnetospheric ring currents, described by a magnetodisc model (Connerney *et al*. 1981). The position of the auroral oval on the surface of the planet is largely dictated by the internal field model, whereas the size of the oval, and the mapping between magnetic colatitude and radial distance, is dictated largely by the magnetodisc model. Until recently, the accuracy of the internal magnetic field model was a serious limitation, leading to uncertainties of *ca.* ±10° latitude in the predicted position of the Io footprint (e.g. Connerney 1992). This meant that the model position of the auroral ovals was uncertain by this amount, leading to difficulties interpreting the early auroral images (see, for example, Caldwell *et al.* 1992; Gérard *et al.* 1993, 1994).

The discovery of an emission feature at the instantaneous foot of the Io Flux Tube (IFT) in images of jovian H_3^+ aurora (Connerney *et al.* 1993) resolved the mapping problem, in large part. Such images are, in effect, self-calibrating. Each observation of the IFT footprint is a fiducial marker, identifying a specific latitude and longitude on Jupiter's surface with a known equatorial radial distance, Io's orbital radial distance of $5.9R_\mathrm{j}$. One could simply measure the angular separation between auroral emissions and the IFT footprint and infer the correct magnetic latitude for the auroral emissions and (with the help of the magnetodisc model) the corresponding source region in the magnetosphere. Over the last few years, many IFT footprints were observed in the IR and UV (Clarke *et al.* 1996, 1998; Prangé *et al.* 1998), leading to a new and improved jovian internal magnetic field model (Connerney *et al.* 1998). The mapping error for the IFT footprint has been reduced to *ca.* 1 or 2° in latitude, equal to the estimated error in location of the IFT footprint in current IR (NASA IRTF) and UV (HST) imagery. At higher magnetic latitudes, mapping to the more distant magnetosphere, accuracy may be limited by time variations and local time variations that are not yet accounted for in the magnetospheric models.

Figure 3*a*, *b* shows H_3^+ emissions in the jovian polar regions. The mapping between the ionosphere and the distant magnetosphere can be visualized by reference to the dotted lines, which trace out the ionospheric footprints for several equatorial radial distances. The spatial distribution of H_3^+ emissions can be inferred from many such images obtained through 360° of jovian rotation. Satoh and co-workers (Satoh *et al.* 1996; Satoh & Connerney 1999*a*) used a detailed emission model and a powerful inverse technique to deduce several important characteristics of the emission. The model uses the bands illustrated in figure 3 to organize polar emissions, allowing for system III and local-time variability within each zone. The 'main oval', representing the most intense emissions, is found within the 12–30R_j band, indicating an origin in what has traditionally been called the middle magnetosphere. Weaker emissions are found to be distributed within the $30R_\mathrm{j}$ oval (mapping to the distant magnetosphere, beyond $30R_\mathrm{j}$ radial distance) and equatorward of the main oval.

Main-oval emissions maximize near system III longitudes of 260° in the north and 130° in the south, corresponding to minima in the magnetic field magnitude. Between the $8R_\mathrm{j}$ and $12R_\mathrm{j}$ ovals, emission peaks at 215° in the north and 25° in the south. This is where the surface magnetic field begins to decrease for electrons drifting azimuthally towards higher system III longitudes in Jupiter's magnetic field. This kind of longitudinal variation of the emission pattern (called the 'windshield-wiper' effect) can be expected (Dessler & Hill 1979; Dessler & Chamberlain 1979; Prangé & Elkhamsi 1991) if the precipitating particles responsible for the energy deposition are drawn from a trapped population. The location of the peak H_3^+ emissions suggests that trapped electrons suffering slow pitch-angle diffusion (compared with an azimuthal drift period) are responsible for the 8–12R_j emissions. In the 12–30R_j band, an isotropic distribution of rapidly pitch-angle scattered electrons is implicated (Satoh *et al.* 1996; Satoh & Connerney 1999*a*). The probability of precipitation for such particles is inversely proportional to the surface field magnitude.

MATHEMATICAL, PHYSICAL & ENGINEERING SCIENCES
THE ROYAL SOCIETY A
PHILOSOPHICAL TRANSACTIONS OF

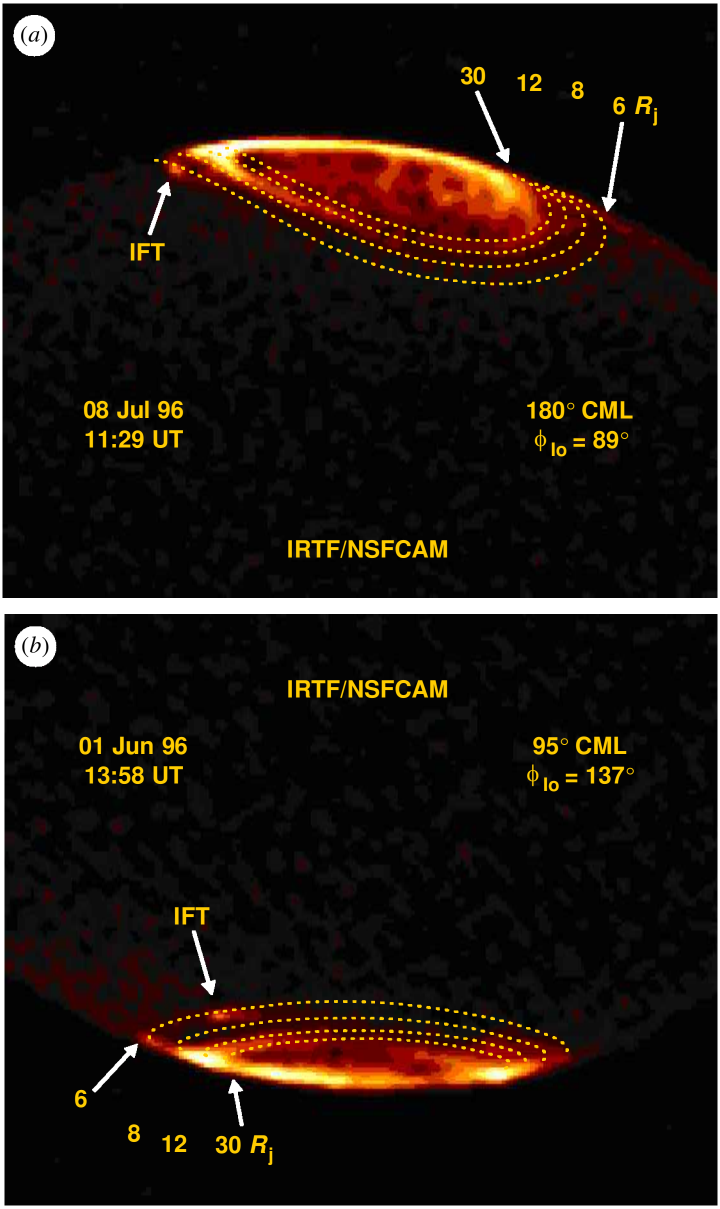

Figure 3. Image of the north (*a*) and south (*b*) polar regions of Jupiter at a wavelength of 3.4 μm showing H_3^+ emissions. Dotted lines indicate the ionospheric footprint of field lines crossing the Equator at radial distances of 6, 8, 12 and 30R_j.

Polar cap H_3^+ emissions (greater than 30R_j) are significantly more intense in the evening sector (Satoh *et al.* 1996; Satoh & Connerney 1999*a*), as are the UV emissions (Clarke *et al.* 1996, 1998). These emissions occur on field lines that extend to large radial distances, where the asymmetry imposed by the solar-wind interaction with Jupiter's magnetosphere becomes apparent. Time variations of auroral intensity

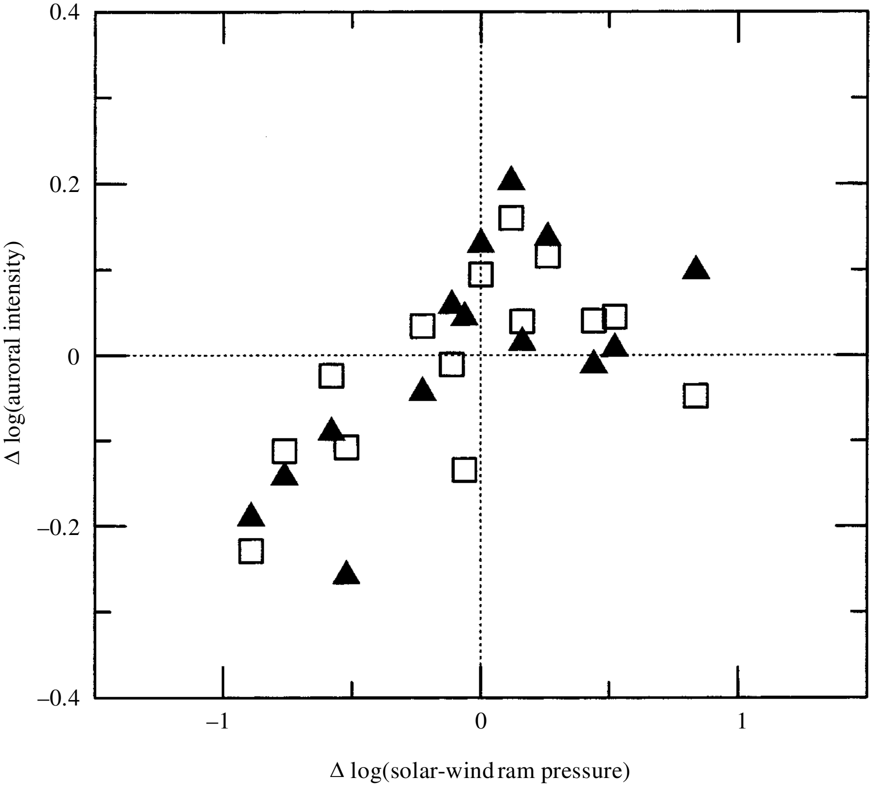

Figure 4. Change (relative to the previous observation) in the total integrated intensity of the aurora as a function of the change in solar-wind ram pressure. Open symbols are used for the northern aurora, filled symbols for the southern aurora.

are observed to co-vary with variations in the solar-wind ram pressure arriving at Jupiter (Baron *et al*. 1996; Connerney *et al*. 1996), with increased auroral emissions observed during periods of increasing solar-wind pressure (figure 4). This observation is consistent with 'magnetic pumping', a process by which charged particles are collectively energized by fluctuations of the magnetic field (Alfvén 1963; Goertz 1978). Since the efficacy of this process depends on the relative magnitude of the field fluctuations ($\delta B/B$), it should be most effective in the distant magnetosphere (beyond 20 or $30R_{\mathrm{j}}$), where a few nT of δB associated with variations in solar-wind ram pressure are a significant fraction of the ambient field strength (Connerney *et al*. 1981). This process also requires relatively rapid pitch-angle scattering, otherwise the energy gained during an increase in the magnetic field is reversibly extracted upon relaxation of the field to its former value.

4. Io interaction

A remarkable relationship between Jupiter and Io became apparent in the 1960s when Bigg (1964) discovered that the observation of high-frequency (22 MHz) radio signals from Jupiter was strongly correlated with Io's orbital phase. Reception is greatly increased when Io's orbital phase (measured from geocentric superior conjunction

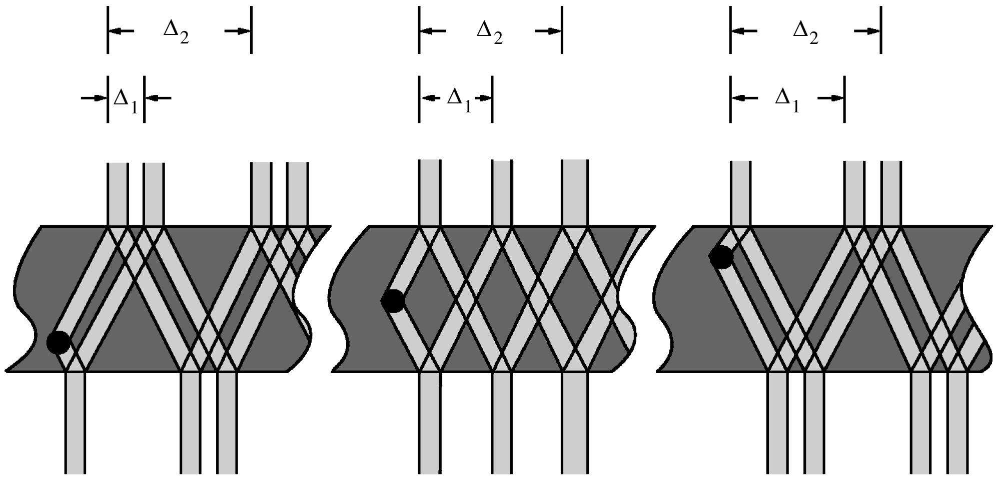

Figure 5. Propagation of Alfvèn waves generated by Io's passage through Jupiter's magnetosphere. Alfvèn waves propagate relatively slowly northward and southward through the high-density plasma torus and may be partly reflected at density gradients in the torus or in Jupiter's ionosphere.

in the direction of Io's orbital motion) is near 90° or 240°. This peculiarity was attributed to an electromagnetic interaction between Jupiter and Io that ultimately gives rise to radio emission from the foot of the IFT (Goldreich & Lynden-Bell 1969; Piddington & Drake 1968). Jupiter's magnetic field sweeps past Io at *ca.* 57 km s^{-1}, generating a motional electric field ($\boldsymbol{V} \times \boldsymbol{B}$) that drives electrical currents along field lines to and from Jupiter's ionosphere. Radio emission is generated at the foot of the IFT, beamed into space along the surface of a hollow cone (the axis of the cone aligns with B and the cone half-angle is *ca.* 75°). The emission is visible when the narrow conical beam sweeps past an observer near the jovigraphic equator.

In Goldreich & Lynden-Bell's (1969) model, the lack of symmetry in the observation of radio waves from Earth is explained by the twist imposed upon the IFT by a few times 10^6 A of current flowing in the flux tube, closing in Jupiter's ionosphere. The essential feature of this DC circuit model is the current closure in the ionosphere. The ionospheric footprint of the IFT 'leads' that of an undisturbed flux tube (one carrying no current) by *ca.* 10° for every 10^6 A of current carried by the flux tube and closing in the ionosphere. Changes in the circuit must be communicated by Alfvèn waves travelling at the Alfvèn velocity. The DC circuit model is applicable only if an Alfvèn wave can propagate from Io to Jupiter and back again before the flux tube slips past Io.

More recent theoretical models favoured an 'open-loop' Io interaction, in which the two-way Alfvèn wave travel time is too great to allow for current closure (Neubauer 1980; Bagenal 1983). In this case, Alfvèn waves radiate away into space (figure 5) and may experience multiple reflections at density gradients in the torus or in Jupiter's ionosphere. The angle of propagation of the Alfvèn wave (with respect to B) depends on the density of the medium through which it propagates. Without current closure, the maximum 'lead' of the foot of the flux tube is at most a few degrees, depending on how much high-density torus the wave propagates through before arriving at Jupiter. The Alfvèn wave model allows for many reflections within the torus and between the torus and Jupiter's ionosphere (Neubauer 1980), creating a standing-wave pattern that originates at Io and extends around the planet. This model was proposed to explain the longitude range and periodic nature of Io-related decametric radio emission (Gurnett & Goertz 1981), the details of which are still poorly understood (Bagenal & Leblanc 1988).

The observation of H_3^+ emission at the instantaneous foot of the IFT (Connerney *et al*. 1993) provided a new and powerful diagnostic for the Io interaction and Jupiter's magnetosphere. The first direct measurements of the position of the IFT footprint confirmed a 'lead' of between 15 and 20°, in accord with Goldreich & Lynden-Bell's (1969) DC circuit model (Connerney *et al*. 1993). In the following years, literally hundreds of IFT footprint observations have been accumulated, mostly in H_3^+ IR imagery but also in the UV (Clarke *et al*. 1996, 1998; Prangé *et al*. 1996, 1998). These have been put to use in improving models of Jupiter's magnetic field (Connerney *et al*. 1998) and in studying the Io interaction.

Recent observations of the IFT footprint (J. E. P. Connerney *et al*., unpublished data) have revealed multiple emission features not unlike those expected of multiply reflected Alfvèn waves propagating downstream of Io (figure 6). In this example, one can see as many as five equally spaced peaks in the H_3^+ emission extending along the Io footprint in the downstream direction. At 110° system III longitude, Io is near the centre of the plasma torus at this time, so one would expect a pattern of equally spaced Alfvèn waves in both hemispheres (see middle section of figure 5). An image of the southern hemisphere at this time shows two distinct emission features separated by *ca.* 4° longitude. We have now observed several such examples, all in the last two years (1998 and 1999). These intensity variations are small and difficult to resolve spatially. It may well be that they have been observed in the last two years as a result of improvements to our observing programme. These include the introduction of narrow-band fixed-wavelength H_3^+ filters on NSFCAM in 1997 and image quality improvements at the IRTF during the same time. However, one cannot dismiss the possibility that the nature of the Io interaction has changed in response to long-term changes in the density of the plasma torus. An increased plasma density in 1998 and 1999 would favour observation of multiply reflected Alfvèn waves (over some Io longitudes).

Evidently, over some Io longitudes, and possibly at some times, the Io interaction is 'closed loop', like that described by Goldreich & Lynden-Bell (1969). At such times, a closed current loop exists and a substantial 'lead' of the IFT footprint may be observed. Over other Io longitudes, and possibly at other times, the interaction is 'open loop'. The Alfvèn wave cannot propagate from Io to Jupiter's ionosphere and back again in time to close the loop. What is lacking at present is a theory that encompasses both behaviours and the transition between them.

Remote observation of the IFT footprint can, thus, be used as a diagnostic of Jupiter's magnetosphere. In principle, the separation between multiple reflections of the IFT can be monitored as a measure of plasma density in the torus. Likewise, in the closed-loop mode, the intensity and position of the IFT footprint communicates information on the electrical current closing in the ionosphere and on power dissipation in the ionosphere. The electron beam itself can be used to probe Jupiter's ionosphere. Approximately 500 000 MW of power are deposited at the foot of the IFT (Goldreich & Lynden-Bell 1969).

PHILOSOPHICAL TRANSACTIONS OF THE ROYAL SOCIETY A MATHEMATICAL, PHYSICAL & ENGINEERING SCIENCES

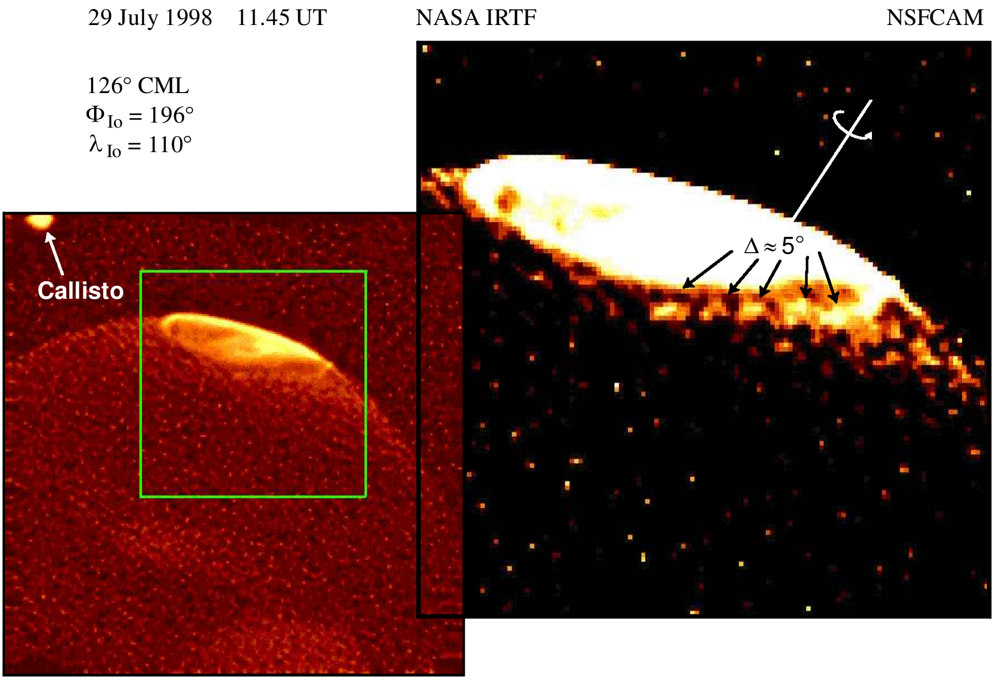

Figure 6. Image of the north polar region of Jupiter at a wavelength of 3.4 μm showing multiple H_3^+ emission features extending downstream (in the plasma flow direction) of the IFT footprint.

5. Summary

The H_3^+ ion has emerged as a very useful probe of Jupiter and its environment, and, most particularly, the interaction between Jupiter's magnetic field and the satellite Io. This tool has been used to improve models of Jupiter's magnetic field; contribute to our understanding of the Io interaction; better understand jovian aurora, the relationship between the aurora and magnetospheric dynamics; and the response of Jupiter's magnetosphere to variations in the solar wind. This is a very promising start for an ion that had not yet been observed, prior to 1988, beyond the Earth.

J.E.P.C. is grateful to The Royal Society and the Novartis Foundation for financial support and the warm hospitality extended during his stay in London. G. Bjoracker at Goddard Space Flight Center supplied the data in figure 1 showing absorption due to methane in Jupiter's atmosphere. We thank S. Miller for helpful discussions. We are pleased to acknowledge the expert assistance of IRTF telescope operators D. Griep, W. Golish and C. Kaminski. We also thank R. Joseph and the staff of the Institute for Astronomy at the University of Hawaii which operates the IRTF for NASA. J.E.P.C. and T.S. are visiting astronomers at the IRTF.

References

Achilleos, N., Miller, S., Tennyson, J., Aylward, A. D., Meuller-Wodarg, I. & Rees, D. 1998 JIM: a time-dependent, three-dimensional model of Jupiter's thermosphere and ionosphere. *J. Geophys. Res.* **103**, 20 089–20 112.

Acuña, M. H., Behannon, K. W. & Connerney, J. E. P. 1983 The main magnetic field of Jupiter. In *Physics of the jovian magnetosphere* (ed. A. J. Dessler), pp. 1–50. Cambridge University Press.

Alfvén, H. 1963 *Cosmical electrodynamics*. Oxford University Press.

Bagenal, F. 1983 Alfvèn wave propagation in the Io plasma torus. *J. Geophys. Res.* **88**, 3013–3025.

Bagenal, F. & Leblanc, Y. 1988 Io's Alfvèn wave pattern and the jovian decametric arcs. *Astron. Astrophys.* **197**, 311–319.

Baron, R., Joseph, R. D., Owen, T., Tennyson, J., Miller, S. & Ballester, G. E. 1991 Imaging Jupiter's aurorae from H_3^+ emissions in the 3–4 μm band. *Nature* **353**, 539–542.

Baron, R., Owen, T., Connerney, J. E. P., Satoh, T. & Harrington, J. 1996 Solar wind control of Jupiter's H_3^+ aurorae. *Icarus* **120**, 437–442.

Bigg, E. K. 1964 Influence of the satellite Io on Jupiter's decametric emission. *Nature* **203**, 1008–1010.

Broadfoot, A. L. *et al.* 1979 Extreme ultraviolet observations from Voyager 1 encounter with Jupiter. *Science* **204**, 979–982.

Burke, B. F. & Franklin, K. L. 1955 Observations of a variable radio source associated with the planet Jupiter. *J. Geophys. Res.* **60**, 213–217.

Caldwell, J., Turgeon, B. & Hua, X.-M. 1992 Hubble Space Telescope imaging of the north polar aurora on Jupiter. *Science* **257**, 1512–1515.

Carr, T. D., Desch, M. D. & Alexander, J. K. 1983 Phenomenology of magnetospheric radio emissions. In *Physics of the jovian magnetosphere* (ed. A. J. Dessler), pp. 226–284. Cambridge University Press.

Clarke, J. T., Moos, H. W., Atreya, S. K. & Lane, A. L. 1980 Observations from Earth and variability of the polar aurora of Jupiter. *Astrophys. J. Lett.* **241**, L179–L182.

Clarke, J. T. *et al.* 1996 Far-ultraviolet imaging of Jupiter's aurora and the Io 'footprint' with the Hubble Space Telescope wide field planetary camera 2. *Science* **274**, 404–409.

Clarke, J. T. *et al.* 1998 HST imaging of Jupiter's UV aurora during the Galileo mission. *J. Geophys. Res.* **103**, 20 217–20 236.

Connerney, J. E. P. 1992 Doing more with Jupiter's magnetic field. In *Planetary radio emissions* (ed. H. O. Rucker & S. J. Bauer), vol. III, pp. 13–33. Vienna: Austrian Academy of Sciences Press.

Connerney, J. E. P. 1993 Magnetic fields of the outer planets. *J. Geophys. Res.* **98**, 18 659–18 679.

Connerney, J. E. P., Acuña, M. H. & Ness, N. F. 1981 Modeling the jovian current sheet and inner magnetosphere. *J. Geophys. Res.* **86**, 8370–8384.

Connerney, J. E. P., Baron, R., Satoh, T. & Owen, T. 1993 Images of excited H_3^+ at the foot of the Io Flux Tube in Jupiter's atmosphere. *Science* **262**, 1035–1038.

Connerney, J. E. P., Satoh, T. & Baron, R. 1996 Interpretation of auroral 'light curves' with application to Jupiter's H_3^+ aurorae. *Icarus* **122**, 24–35.

Connerney, J. E. P., Acuña, M. H., Ness, N. F. & Satoh, T. 1998 New models of Jupiter's magnetic field constrained by the Io Flux Tube footprint. *J. Geophys. Res.* **103**, 11 929–11 939.

Dessler, A. J. & Chamberlain, J. W. 1979 Jovian longitudinal asymmetry in Io-related and Europa-related auroral hot spots. *Astrophys. J.* **230**, 974–981.

Dessler, A. J. & Hill, T. W. 1979 Jovian longitudinal control of Io-related radio emissions. *Astrophys. J.* **227**, 664–675.

Dols, V., Gerard, J. C., Paresce, F., Prangé, R. & Vidalmadjar, A. 1992 Ultraviolet imaging of the jovian aurora with the Hubble Space Telescope. *Geophys. Res. Lett.* **19**, 1803–1806.

Drossart, P. (and 11 others) 1989 Detection of H_3^+ on Jupiter. *Nature* **340**, 539–541.

Gérard, J.-C., Dols, V., Paresce, F. & Prangé, R. 1993 Morphology and time variation of the jovian far UV aurora: Hubble Space Telescope observations. *J. Geophys. Res.* **98**, 18 793–18 801.

Gérard, J.-C., Dols, V., Prangé, R. & Paresce, F. 1994 The morphology of the north jovian ultraviolet aurora observed with the Hubble Space Telescope. *Planet. Space Sci.* **42**, 905–917.

Goertz, C. K. 1978 Energization of charged particles in Jupiter's outer magnetosphere. *J. Geophys. Res.* **83**, 3145–3150.

Gold, J. 1959 Motions in the magnetosphere of the Earth. *J. Geophys. Res.* **64**, 1219–1224.

Goldreich, P. & Lynden-Bell, D. 1969 Io, a jovian unipolar inductor. *Astrophys. J.* **156**, 59–78.

Gurnett, D. A. & Goertz, C. K. 1981 Multiple Alfvèn wave reflections excited by Io: origin of the jovian decametric arcs. *J. Geophys. Res.* **86**, 717–722.

Kim, Y. H. & Fox, J. L. 1994 The chemistry of hydrocarbon ions in the jovian ionosphere. *Icarus* **112**, 310–325.

Kim, S. J., Drossart, P., Caldwell, J., Maillard, J.-P., Herbst, T. & Shure, M. 1991 Images of aurorae on Jupiter from H_3^+ emission at 4 microns. *Nature* **353**, 536–539.

Lam, H. A., Achilleos, N., Miller, S. & Tennyson, J. 1997 A baseline spectroscopic study of the infrared auroras of Jupiter. *Icarus* **127**, 379–393.

Leu, M. T., Bondi, M. A. & Johnsen, R. 1973 Measurements of recombination of electrons with H_3^+ and H_5^+. *Phys. Rev.* A **8**, 413–419.

Miller, S., Joseph, R. D. & Tennyson, J. 1990 Infrared emission of H_3^+ in the atmosphere of Jupiter in the 2.1 and 4.0 micron region. *Astrophys. J.* **360**, L55–L58.

Miller, S., Achilleos, N., Ballester, G. E., Lam, H. A., Tennyson, J., Geballe, T. R. & Trafton, L. M. 1997 Mid to low latitude H_3^+ emission from Jupiter. *Icarus* **130**, 57–67.

Neubauer, F. M. 1980 Nonlinear standing Alfvèn wave current system at Io: theory. *J. Geophys. Res.* **85**, 1171–1178.

Oka, T. & Geballe, T. R. 1990 Observations of the 4 micron fundamental band of H_3^+ in Jupiter. *Astrophys. J.* **351**, L53–L56.

Piddington, J. H. & Drake, J. F. 1968 Electrodynamic effects of Jupiter's satellite Io. *Nature* **217**, 935–937.

Prangé, R. & Elkhamsi, M. 1991 Modeling the precipitation flux in the jovian auroral zones. I. The model and its application to the UV auroral emissions. *J. Geophys. Res.* **96**, 21 371–21 389.

Prangé, R., Rego, D., Southwood, D., Zarka, P., Miller, S. & Ip, W.-H. 1996 Rapid energy dissipation and variability of the Io–Jupiter electrodynamic circuit. *Nature* **379**, 323–325.

Prangé, R. *et al.* 1998 Detailed study of FUV jovian auroral features with the post-COSTAR HST faint object camera. *J. Geophys. Res.* **103**, 20 195–20 216.

Satoh, T. & Connerney, J. E. P. 1999*a* Jupiter's H_3^+ emissions viewed in corrected Jovimagnetic coordinates. *Icarus* **141**, 236–252.

Satoh, T. & Connerney, J. E. P. 1999*b* Spatial and temporal variations of Jupiter's H_3^+ emissions deduced from image analysis. *Geophys. Res. Lett.* **26**, 1789–1792.

Satoh, T., Connerney, J. E. P. & Baron, R. 1996 Emission source model of Jupiter's H_3^+ aurorae: a generalized inverse analysis of images. *Icarus* **122**, 1–23.

Strobel, D. F. & Atreya, S. K. 1983 Ionosphere. In *Physics of the jovian magnetosphere* (ed. A. J. Dessler), pp. 51–67. Cambridge University Press.

Trafton, L., Lester, D. F. & Thompson, K. L. 1989 Unidentified emission lines in Jupiter's northern and southern 2 micron aurorae. *Astrophys. J.* **343**, L73–L76.

Waite Jr, J. H., Lewis, W. S., Gladstone, G. R., Cravens, T. E., Maurellis, A. N., Drossart, P., Connerney, J. E. P., Miller, S. & Lam, H. A. 1997 Outer planet ionospheres: a review of recent research and a look to the future. *Adv. Space Res.* **20**, 243–252.

PHILOSOPHICAL TRANSACTIONS OF THE ROYAL SOCIETY A MATHEMATICAL, PHYSICAL & ENGINEERING SCIENCES